

Efficient AI in Practice: Training and Deployment of Efficient LLMs for Industry Applications

Kayhan Behdin*
 Yun Dai*
 Ata Fatahibaarzi*
 Aman Gupta*
 Qingquan Song*
 kbehdin@linkedin.com
 yudai@linkedin.com
 afatahibaarzi@linkedin.com
 amagupta@linkedin.com
 qsong@linkedin.com
 LinkedIn
 Sunnyvale, California, USA

Shao Tang
 Hejian Sang
 Gregory Dexter
 Sirou Zhu
 Siyu Zhu
 Tejas Dharamsi
 Maziar Sanjabi
 Vignesh Kothapalli
 Hamed Firooz
 shatang@linkedin.com
 hsang@linkedin.com
 gdexter@linkedin.com
 sirzhu@linkedin.com
 jzhu@linkedin.com
 tdharamsi@linkedin.com
 maz@linkedin.com
 vkothapalli@linkedin.com
 hfirooz@linkedin.com
 LinkedIn
 Sunnyvale, California, USA

Zhoutong Fu
 Yihan Cao
 Pin-Lun Hsu
 Fedor Borisyyuk
 Zhipeng Wang
 Rahul Mazumder
 Natesh Pillai
 Luke Simon
 zfu@linkedin.com
 yihacao@linkedin.com
 byhsu@linkedin.com
 fborisyu@linkedin.com
 zhipwang@linkedin.com
 rmazumder@linkedin.com
 npillai@linkedin.com
 lsimon@linkedin.com
 LinkedIn
 Sunnyvale, California, USA

Abstract

Large language models (LLMs) have demonstrated remarkable performance across a wide range of industrial applications, from search and recommendations to generative tasks. Although scaling laws indicate that larger models generally yield better generalization and performance, their substantial computational requirements often render them impractical for many real-world scenarios at scale. In this paper, we present methods and insights for training small language models (SLMs) that deliver high performance and efficiency in deployment. We focus on two key techniques: (1) knowledge distillation and (2) model compression via quantization and pruning. These approaches enable SLMs to retain much of the quality of their larger counterparts while significantly reducing training, serving costs, and latency. We detail the impact of these techniques on a variety of use cases at a large professional social network platform and share deployment lessons—including hardware optimization strategies that enhance speed and throughput for both predictive and reasoning-based applications.

Keywords

large language models, distillation, pruning, compression, quantization

1 Introduction

Large language models (LLMs) [13, 24, 35, 48] have ushered in a new era in artificial intelligence and machine learning, driving significant improvements in deployed systems across various industries.

LLMs suitable for real-world applications come in diverse forms, differing in size (ranging from hundreds of millions to hundreds of billions of parameters), architectural design (e.g., encoder-based models like BERT [12] versus decoder-based models like GPT-3 [7]), and training paradigms (such as pre-training, instruction tuning, or test-time computation [13, 19, 24, 35, 38, 48]).

In industry, LLMs are deployed to address a multitude of applications:

- **Search:** Enabling embedding generation [53, 54] and semantic ranking and matching [43].
- **Retrieval and Ranking:** Supporting retrieval [60] and ranking of items [14, 33, 34].
- **Generative Use Cases:** Powering applications such as chatbots, assistants, and image generators [1, 11, 46].

Furthermore, scaling laws for LLMs have established a strong correlation between model size, validation loss, and downstream task performance [22, 26, 44, 55]. As a result, increasing the model size is often one of the most effective strategies for enhancing performance. Modern LLMs, particularly autoregressive decoder-only models, have expanded to hundreds of billions of parameters.

While large LLMs exhibit high performance, deploying such large models incurs substantial infrastructure costs, especially for latency- or throughput-sensitive tasks. However, both academia and industry have developed strategies for creating and deploying

*Authors contributed equally to this research, sorted by last name

efficient small language models (SLMs). Here, we primarily focus on methods which leverage an existing internally trained large LLM to create an efficient SLM that largely maintains the original model’s accuracy. Approaches to achieve this include white-box or black-box distillation [2, 17, 21, 25, 51], compression techniques such as quantization [4, 16] or sparsification [15, 36, 37, 47].

In this work, we present a comprehensive set of lessons learned from developing and deploying various SLMs into production at a large-scale social networking company. We address a wide array of predictive and generative use cases, with inference performance and latency constraints in serving as key considerations. Specifically, our contributions are as follows:

- We discuss several large-scale use cases for which language models are useful.
- For these use cases, we explore techniques for developing tailored SLMs, with a focus on knowledge distillation and model compression methods such as quantization and structured pruning.
- We discuss inference, latency, and other serving considerations, offering insights into the infrastructure required to reliably deploy SLMs in high-throughput or low-latency production environments, and share practical lessons from our real-world deployments.

We apply these methods to the following real-world use cases, with experimental results and discussion provided in Section 4:

- **SLM for predictive tasks obtained through distillation and pruning** - We leverage a foundation model (FM) for ranking and recommendations [14, 33] and leverage distillation and pruning to create an SLM that is efficient for serving latency-sensitive use cases. The final SLM we create is more than 20× smaller without any appreciable loss in quality.
- **SLM for reasoning task obtained through distillation** - We leverage various flavors of KD to compress a latency-sensitive reasoning model by more than 5× without any appreciable loss in quality.

The remainder of the paper is organized as follows. In Section 2, we review related work. Section 3 details the efficiency techniques employed for creating, modifying, and deploying SLMs. Section 4 presents experimental results. We then address practical deployment considerations in Section 5 and conclude with a discussion of our findings and suggestions for future research.

2 Related work

Research on efficient LLMs has extensively explored pruning, knowledge distillation, and quantization. Muralidharan et al. [39] investigate pruning and distillation to maintain performance in smaller models. The Minitron paper [40] focuses on advanced pruning for deployment, while Apple’s study [18] integrates multiple techniques, including quantization, for efficiency. Insights on hyperparameter tuning [3, 42] offer valuable training guidance but lack focus on compression or deployment, and surveys like [63] provide overviews without empirical validation. In contrast, our work emphasizes lessons on efficiency through distillation and compression, coupled with practical deployment considerations such as inference optimization and GPU capacity utilization. With hundreds

of millions of users worldwide, our use cases require models that efficiently handle large-scale data and deliver personalized, relevant content tailored to professional networking functionalities. We focus on fine-tuning language models specifically for industry use cases, ensuring alignment with our unique requirements and optimizing models for high-demand, real-world environments. This application-driven approach not only bridges the gap between theoretical compression methods and practical deployment needs but also provides actionable insights on optimizing GPU usage and deployment strategies. By addressing both efficiency and deployment challenges, our research distinguishes itself from more generalized studies, offering tangible solutions for large-scale social networks.

3 Methods

In this section, we detail various techniques that allow SLMs to retain strong generalization or task-specific performance, while allowing efficient serving from a latency or throughput standpoint. Specifically, we discuss training via knowledge distillation and post-training model compression. We also intersperse serving and training efficiency concerns throughout the write-up.

3.1 Knowledge Distillation

Modern LLMs work with tokens as the currency of input and output. Let $\mathbf{x} = [x_1, x_2, x_3, \dots]$ represent an input prompt consisting of a sequence of tokens. Given this prompt, a large language model (LLM) generates a response $\mathbf{y} = [y_1, y_2, y_3, \dots, y_T]$, producing tokens sequentially in an autoregressive manner. An LLM models the probability distribution $q_\theta(\mathbf{y}|\mathbf{x})$, parametrized by θ .

Knowledge distillation (KD) [21] transfers knowledge from a larger and expressive “teacher” model to a smaller “student” model, allowing the latter to approximate teacher performance with reduced computational resources. KD can be broadly performed in two different ways (1) by leveraging the output of a teacher model to train the student [19, 51] (also known as **black-box** distillation) or (2) by leveraging intermediate outputs [21, 40] (also known as **white-box** distillation). White-box distillation using the soft probabilistic outputs of the teacher is a powerful technique and helps provide richer information than hard labels used in supervised fine-tuning (SFT), helping the student generalize better, especially in tasks where smaller models struggle to discover patterns in noisy data.

We consider white-box KD using a training objective with the following general structure. Formally, given a fixed teacher model distribution $p(\mathbf{y}|\mathbf{x})$, the student model q_θ under the same vocabulary is trained by minimizing the following objective:

$$\mathcal{L}[p_\mathbf{y}, \mathcal{D}(p||q_\theta)] = \mathbb{E}_{\mathbf{x} \sim p_\mathbf{x}} \mathbb{E}_{\mathbf{y} \sim p_\mathbf{y}(\cdot|\mathbf{x})} \left[\sum_{t=1}^T \mathcal{D}(p(\cdot|y_{<t}, \mathbf{x}) || q_\theta(\cdot|y_{<t}, \mathbf{x})) \right] \quad (1)$$

where $p_\mathbf{y}$ denotes the distribution from which the response \mathbf{y} is sampled, \mathcal{D} is a divergence measure between two next-token distributions, and T is the maximum response length. This objective emphasizes two aspects:

- (1) Responses are drawn from $p_\mathbf{y}$, which may correspond to ground truth data, the teacher model (sequence-level KD) [27],

or the student model itself (on-policy KD) [2, 17, 62]. Recent advancements [28, 57] explore a balance between on-policy and off-policy sampling to mitigate the mismatch between student-generated responses and the teacher’s distribution while addressing inefficiencies in online student autoregressive training.

- (2) The student model is optimized to minimize the discrepancy between its next-token distribution q_θ and the teacher’s predictions p , ensuring knowledge transfer across the response sequence.

In this work, we explore different KD strategies based on the task requirements. We also experiment with various student initialization techniques and divergence measures.

Let \mathcal{V} denote the vocabulary. The commonly used divergences are:

- Forward Kullback-Leibler (KL) Divergence (FKL):

$$\mathcal{D}_{\text{FKL}} [p(y_t|y_{<t}, \mathbf{x}) \| q_\theta(y_t|y_{<t}, \mathbf{x})] = \sum_{i \in \mathcal{V}} p(i|\cdot) \log \left(\frac{p(i|\cdot)}{q_\theta(i|\cdot)} \right),$$

- Reverse Kullback-Leibler Divergence (RKL):

$$\mathcal{D}_{\text{RKL}} [p(y_t|y_{<t}, \mathbf{x}) \| q_\theta(y_t|y_{<t}, \mathbf{x})] = \sum_{i \in \mathcal{V}} q_\theta(i|\cdot) \log \left(\frac{q_\theta(i|\cdot)}{p(i|\cdot)} \right),$$

- Jensen-Shannon Divergence (JSD):

$$\mathcal{D}_{\text{JS}(\beta)} [p(y_t|y_{<t}, \mathbf{x}) \| q_\theta(y_t|y_{<t}, \mathbf{x})] = \beta \mathcal{D}_{\text{FKL}} [p \| m] + (1 - \beta) \mathcal{D}_{\text{FKL}} [q_\theta \| m],$$

where $m = \beta p + (1 - \beta) q_\theta$ is the mixture distribution.

3.2 Post-training compression

Model compression is a widely-studied area of machine learning efficiency. We specifically focus on post-training compression (PTC) techniques to improve the inference efficiency of SLMs and LLMs.

Our focus is on post-training compression, where compression is applied to the model after training. Recent compression methods follow a layerwise compression approach (Equation 2) since modern models have ballooned in size and it can be scaled to large models without a major compromise in accuracy.

We now present a mathematical framework for layerwise PTC using calibration data. Let $\mathbf{X} \in \mathbb{R}^{n \times d}$ denote the calibration data that serve as inputs to a linear layer of the model (e.g., an MLP or an attention projection). Here, n is the number of tokens in the calibration dataset, and d is the input dimension of the layer. For instance, in the case of an MLP down projection layer of a Transformer block, d corresponds to the intermediate size of the model.

Furthermore, let $\mathbf{W} \in \mathbb{R}^{d \times p}$ denote the weight matrix of the layer, where p is the output dimension. In the MLP down projection example, p represents the hidden size of the model. We denote by $\hat{\mathbf{W}} \in \mathbb{R}^{d \times p}$ the weight matrix after compression. The layerwise reconstruction error is defined as $\|\mathbf{X}\mathbf{W} - \mathbf{X}\hat{\mathbf{W}}\|_F^2$. Thus, for each layer that undergoes compression, we consider an optimization problem of the form

$$\min_{\hat{\mathbf{W}}} \|\mathbf{X}\mathbf{W} - \mathbf{X}\hat{\mathbf{W}}\|_F^2 \quad \text{subject to} \quad \hat{\mathbf{W}} \in \mathcal{Q}, \quad (2)$$

where $\mathcal{Q} \subseteq \mathbb{R}^{d \times p}$ denotes the set of feasible solutions that conform to a particular compression scheme. In practice, the set \mathcal{Q} often exhibits a discrete structure, which renders the optimization problem in (2) challenging to solve.

Here, we consider two compression techniques:

Quantization In quantization, the model weights are represented in lower precision, using a fewer number of bits. Quantization has proved to be successful in the LLM domain, to obtain compressed models with small accuracy loss [16, 56]. In this work, we consider weight-only quantization, where only model weights are quantized, as well as weight and activation quantization. We study methods such as GPTQ [16] and QuantEase [4] for 4-bit weight-only quantization (aka W4A16), SmoothQuant [56] for 8-bit weight-and-activation quantization (aka W8A8), and 8-bit floating-point (FP8) quantization. Since quantization is dependent on hardware, we discuss the details of quantization-related experiments in Section 5 (deployment).

Structured Pruning Neural network pruning [20, 32] is a post-training compression technique, where some model weights are set to zero, resulting in sparse model weight matrices. Recent years have seen a surge of papers in pruning techniques for LLMs—examples include [15, 36, 47]. Without any structure on the model sparsity, however, it can be difficult to realize any inference acceleration from pruning. Therefore, in this work, we pursue a structured pruning approach. In structured pruning, the goal is to obtain smaller models via removing some neurons from the model weights. In particular, we study MLP pruning, where the goal is to reduce the intermediate size of the model via removing some hidden neurons in feed-forward layers. We also study attention pruning, where we remove a certain number of attention heads from the model [29, 30, 37]. In this paper, we use OSSCAR [37] which uses a discrete optimization approach for structured pruning. OSSCAR can be scaled to large scale problems, which we consider. We leverage OSSCAR because it represents the state-of-the-art when it comes to post-training structured pruning of LLMs and leads to the least drop in accuracy when compared to other methods.

3.3 Training and serving efficiency

Despite significant algorithmic advances, the challenges of training and serving LLMs persist. Efficient training and serving remain critical for practical deployment, requiring ongoing improvements in kernel optimization, distributed training, and inference acceleration.

Training Efficiency LLM training presents a formidable challenge due to the sheer scale of these models and the quadratic complexity of transformer architectures. Model FLOPs utilization (MFU) [8] is commonly used to measure GPU efficiency, making it necessary to optimize kernel operations and distributed training strategies. We have implemented Liger Kernel [23] in Triton [50], incorporating several key optimizations. First, we employ kernel fusion to reduce repetitive memory transfers between SRAM and DRAM. Next, we adopt in-place tensor modifications to avoid creating additional tensors whenever possible, thus lowering the memory footprint. We also apply chunking, which prevents the full materialization of large tensors and provides tuning flexibility while maintaining

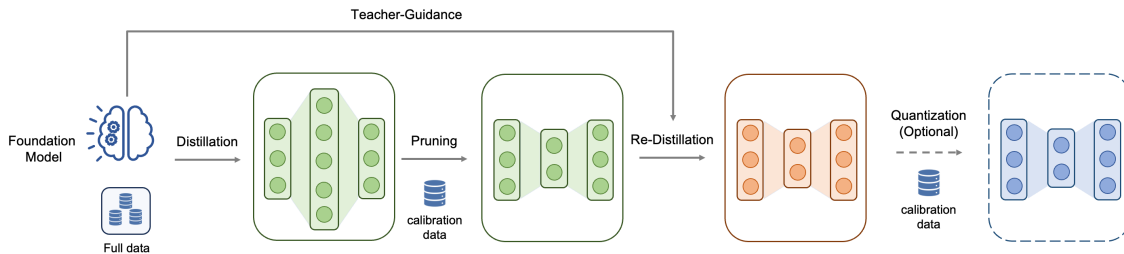


Figure 1: Overview of the process of creating SLMs via distillation and compression.

comparable performance. In combination, these optimizations reduce training time by 20% and memory usage by 60%. Additional performance-memory tradeoffs such as gradient checkpointing and CPU offloading can lead to as much as a threefold speedup.

For distributed training, we use ZeRO [45] to shard model parameters and data across multiple GPUs, overlapping computation with communication to sustain high MFU. Together with the DeepSpeed team, we have optimized the ZeRO algorithm, and for network-constrained clusters, we have developed ZeRO++ [10, 52] to mitigate non-deterministic synchronization issues that can hinder convergence. ZeRO++ provides a 2.4× speedup over vanilla ZeRO.

Serving Efficiency Serving LLMs efficiently poses unique challenges due to both high computational demands and strict latency requirements. In production environments, the choice of a serving framework is pivotal for maximizing throughput and minimizing response times. Several solutions, including vLLM, SGLag, TRT-LLM, and MLC-LLM [31, 41, 49, 61], have been proposed to address these needs. In our use cases, we evaluated vLLM and SGLang extensively. Our benchmarks revealed that SGLang is better suited to our workloads because its radix tree-based caching mechanism aligns well with our usage patterns and it integrates tightly with FlashInfer [59], whose efficient attention kernels accelerate the sequence lengths and batch sizes we typically handle.

To further improve serving performance, we deploy our models on NVIDIA H100 GPUs at FP8 precision, striking a practical balance between computational efficiency and model quality. Additional details regarding the serving engine configurations for our experiments can be found in Section 5.

4 Experiments

4.1 Setup

Training details We consider models ranging in size from a billion to ~ 100B parameters. For all use cases, we appropriately tune the learning rate, learning rate warmup schedule and decay, as well as weight decay. Context length varies from a few hundred tokens to up to 32k, depending on the use case. We provide use-case specific details at the appropriate place.

Prompt Structures For predictive tasks, we are mainly interested in ranking use cases. Hence, the use of decoder-based LLMs is prefill-dominant. For generative and reasoning based-tasks, we are

also interested in decoding latencies. We relegate the details of the prompt structures to subsections discussing the specific use cases. **Quality metrics** We use different accuracy measures across tasks. For predictive tasks, we use area under the curve (AUC). For generative tasks, we rely on validation loss and task-specific metrics.

4.2 Foundational model for RecSys

4.2.1 Problem setup. We base our experiments on an internal foundation model (FM) trained using text, primarily for the purpose of ranking and recommendations [14]. The FM consists of 100B+ parameters and is trained to approximate the following distribution for a large variety of recommendation tasks where users interact with items:

$$P(m, (e_1, t_1), \dots, (e_T, t_T)), \quad (3)$$

where m represents a user, and each pair (e_t, i_t) for $t = 1, \dots, T$ represents the user’s interaction i_t (like or click or equivalent) with an entity e_t (such as post on a social media platform). As mentioned before, the featurization is performed purely via text, allowing the FM to effectively generalize across heterogeneous tasks. The model is then used to estimate the following probabilities for future interactions with entities:

$$P(i_t, i_{t+1}, \dots | \text{Task instruction}, m, (e_1, i_1), \dots, (e_{t-1}, i_{t-1}), e_t, e_{t+1}, \dots) \quad (4)$$

Text-based featurization makes decoder-only LLMs an attractive option for training this model jointly on a large and varied of recommendation tasks. The FM uses single-token generation for pointwise ranking and probability estimation. The reader is encouraged to peruse [14] for more details about the FM.

Due to the large size of the FM—which contains over 100 billion parameters—serving it online for latency-sensitive applications is challenging. In this work, we present experiments demonstrating how we achieved a more than 20× reduction in model size, enabling the online serving of a distilled version of the FM with only a modest loss in accuracy.

Our approach, illustrated in Figure 1, proceeds in three stages: 1) **Distillation** on the full model. 2) **One-shot pruning**¹ to significantly reduce the model size. 3) **Re-distillation** of the pruned

¹“One-shot” indicates pruning without any re-training.

model to recover generalization capabilities. All distillation is performed in a post-training setting using data from various recommendation tasks. We optionally also quantize the model (details in Section 5). We measure quality by reporting the AUC on the test sets of in-domain tasks, computing AUC per task and then averaging across tasks.

4.2.2 Distillation Results. To evaluate how knowledge distillation (KD) affects model generalization, we compare it against standard supervised fine-tuning (SFT). We focus on the task performance retention of the distilled (or fine-tuned) student models relative to the original foundation model (FM). Specifically, we use Llama-3.1-8B-Instruct and Llama-3.2-3B-Instruct [13] as our student models. These models offer strong performance while remaining sufficiently compact for throughput- and latency-sensitive environments. In both KD and SFT, responses are generated from the ground-truth action-prediction labels.

For KD, the per-token loss is a weighted combination of: 90% forward KL divergence between teacher and student logits, and 10% cross-entropy loss with the ground-truth labels.

Additionally, we include an extra 5% loss contribution computed over the entire sequence (including the prompt), normalized by its token count. Thus, 95% of the loss is computed solely on action prediction tokens, while the remaining 5% is computed over the prompt tokens.

Each KD and SFT configuration undergoes hyperparameter tuning (e.g., peak learning rate, warmup schedule, decay schedule, and weight decay). Figure 2 summarizes the results by reporting the AUC delta relative to the original FM (which achieves the best performance). The main observations are as follows:

- **SFT:** The 3B and 8B student models fine-tuned only with SFT underperform compared to the FM, which is expected given their smaller size and post-training. The performance drop for the 3B model (-1.21%) is larger than that of the 8B model (-0.62%).
- **KD:** Using logit supervision from the FM consistently preserves task performance better than SFT. The 8B-KD model shows a minor AUC drop of -0.06% (compared to -0.62% for 8B-SFT), while the 3B-KD model (-0.15%) substantially mitigates the loss relative to 3B-SFT (-1.21%). These results demonstrate the effectiveness of KD for transferring knowledge, allowing smaller models to remain competitive.

Overall, KD performs well on transferring the knowledge from the teacher model and improving smaller model’s generalization performance, enabling us to compress a 100B+ FM into smaller models with 3B and 8B parameters.

4.2.3 Post-training Compression Results. After obtaining the distilled student models, we apply structured pruning and on-the-fly FP8 quantization to further compress the model to meet our serving latency requirements (steps outlined in Figure 1). Since the distilled models (DMs) are decoder-only transformers, our approach focuses on applying structured pruning to remove redundant MLP up/down projection neurons, as well as attention heads in each transformer layer while preserving its capabilities on in-domain ranking tasks. Since one-shot pruning results in loss in quality, we apply targeted fine-tuning after each pruning step to ensure that the model adapts

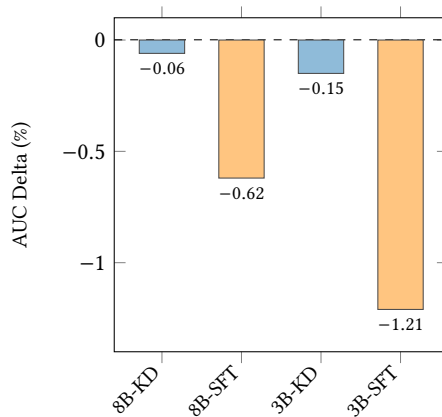


Figure 2: Comparison of Distillation and SFT on the Foundation Model. Knowledge distillation consistently outperforms SFT by effectively leveraging teacher supervision to preserve and enhance performance.

to its reduced size without significant performance loss. To this end, we again leverage knowledge distillation to bridge the gap between the original and pruned models, transferring key insights and ensuring the pruned version closely aligns with the outputs of the original foundational model.

For structured pruning, we leverage the OSSCAR algorithm [37]. We now discuss the details of various ablations that we conducted towards structured pruning.

Effect of SFT vs. distillation As illustrated in Figure 1, we employ OSSCAR to prune the distilled model in a layerwise fashion. After pruning, we use either SFT or KD to restore any lost generalization, with the unpruned distilled model serving as the teacher. To demonstrate the effectiveness of each approach, we examine an 8B distilled model and its 6.4B pruned counterpart (i.e., 20% pruning of the MLP layers). Table 1 presents the results. Consistent with the findings for pure distillation, the pruned model benefits significantly more from KD than from SFT. Results for the 3B model (pruned to 2.4B) mirror this trend and are omitted for brevity.

While SFT offers a more straightforward optimization path, distillation provides additional flexibility by leveraging teacher–student training to refine model weights more effectively. In practice, the choice of distillation algorithms and associated losses (e.g., forward KL combined with SFT loss) may vary depending on data availability, computational constraints, and the chosen pruning ratio. Nevertheless, in most cases, including a forward KL term proves highly beneficial in counteracting the performance drop associated with pruning.

Pruning the 8B and 3B distilled models down to 6.4B and 2.4B, respectively, can yield further improvements in serving efficiency. Additional details on deployment are provided in Section 5.

Effect of degree and schedule of pruning We next investigate how varying the pruning ratio impacts downstream task accuracy. Table 2 reports one-shot pruning results (i.e., no SFT or KD is applied post-pruning) on an 8B model that has undergone an SFT stage (based on Llama-3.1-8B-Instruct) comparable to the foundation model. As expected, more aggressive pruning reduces model size

Model	AUC Delta (%)
8B Distilled Model	-
6.4B Pruned Model (20%) + SFT	-0.47%
6.4B Pruned Model (20%) + Distillation	-0.06%

Table 1: Distillation vs. SFT for post-pruning retraining. The pruned model has its MLP layers pruned by 20%.

Model	AUC Delta (%)
8B Model	-
6.8B Pruned Model	0.0%
6.4B Pruned Model	-1.33%
6.0B Pruned Model	-1.72%

Table 2: Evaluation of the 8B-parameter model post-SFT and its pruned variants, focusing on MLP pruning performed in a one-shot manner (i.e., no retraining after pruning).

Model	#Params	AUC Delta (%)
3B (Distilled from FM)	3B	-
MLP Prune + Distill	2.4B	-0.12%
MLP Prune + Distill (Gradual)	2.4B	0.03%

Table 3: Comparison of one-step vs gradual pruning for a 3B model distilled from the FM.

but also significantly degrades task accuracy. Notably, small pruning ratios (e.g., from 8B to 6.8B) have minimal effect on performance, while heavier pruning leads to larger accuracy drops. However, as shown in Table 1, such performance losses can be mitigated by applying distillation.

We also explore *gradual pruning* [5] in which the model is pruned in multiple steps, with knowledge distillation after each pruning. Table 3 summarizes results for pruning a distilled 3B model to 2.4B (a 37.5% MLP sparsity) either in a single step or in two smaller steps (removing 1536 hidden neurons in each step, for a total of 3072). The gradual approach recovers model AUC better than the single-step approach, achieving near-lossless compression from 3B to 2.4B.

Finally, to study attention-head pruning, we take the 2.4B model obtained by gradual MLP pruning and prune half of its attention heads via OSSCAR in a one-shot manner, followed by KD. Table 4 shows that one-shot attention pruning incurs a modest quality loss, but the subsequent KD phase restores the model to AUC parity with the 2.4B baseline.

Effect of calibration data Figure 3 captures the effect of the calibration dataset X (discussed in Section 3 and Equation (2)) on the accuracy of the pruned versions of the 8B student model (results for the 3B model are similar and are hence omitted for clarity). The *Full Precision* bar illustrates the baseline accuracy of the non-pruned model. We consider two different datasets for calibration - C4 [44], an open source dataset, and an in-domain dataset. When we prune using a randomly sampled portion of the C4 dataset (1,024 or 4,096

Model	#Params	AUC Delta (%)
MLP Pruning	2.4B	-
\wedge + Attention Pruning	2.1B	-1.07%
\wedge + Distillation	2.1B	0.02%

Table 4: Results for attention pruning. We consider the 2.4B gradual pruning model from Table 3 as the base. The second row shows the result for one-shot attention pruning, while the last row shows the results after performing distillation.

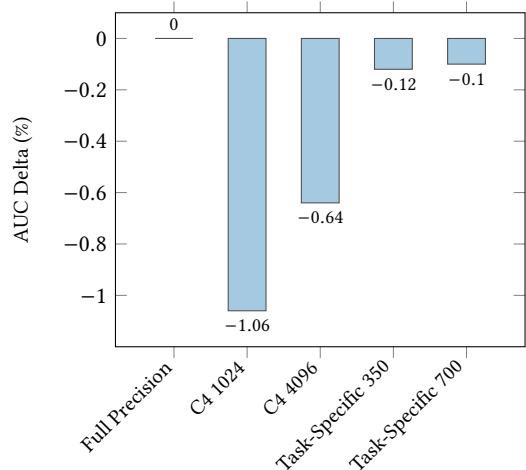


Figure 3: Comparison of one-shot pruning methods. The bars indicate the drop (in percentage points) relative to the full precision baseline. The pruned model is a 6.4B model (20% MLP pruning).

examples), accuracy drops, although more samples mitigate this drop to an extent. These results indicate that increasing the number of calibration examples from 1,024 to 4,096 can partially recover lost accuracy due to pruning. However, leveraging fewer but more domain-specific samples (350 or 700 examples from the target task) yields better accuracy values, which closely match the full precision baseline. This highlights the importance of using task-relevant data for calibration, even if it involves fewer examples, as it can produce more accurately pruned models than generic calibration sets.

4.3 Reasoning Task

We detail experiments for a use case that requires generating reasoning for various input prompts.

4.3.1 Distillation Results. We investigate several distillation methods to produce a 1.5B model initialized from Qwen-2.5-1.5B-Instruct [58]. The teacher models are obtained by training various sizes of Qwen-2.5 Instruct models using SFT with identical hyperparameters. Performance is primarily measured by validation loss, with lower values indicating higher accuracy (see Table 5).

In a single-stage, word-level training setup, the Forward KL (FKL, $\beta = 0$) loss achieves the lowest validation loss, outperforming the Jensen-Shannon Divergence (JSD, $\beta = 0.5$), SFT, and Reverse KL

(RKL, $\beta = 1.0$) approaches. Notably, a larger teacher model does not necessarily lead to superior outcomes; for example, a 3B \rightarrow 1.5B distillation can outperform a 7B \rightarrow 1.5B configuration.

In contrast, a two-stage approach—an initial word-level distillation phase followed by on-policy training with the FKL loss (oFKL)—consistently yields better performance than single-stage training alone. Our experiments show that initializing the second stage with the best checkpoint from the first stage (e.g., an FKL-distilled model) is more effective than starting from either an SFT model or the original, non-SFT model. Additionally, an on-policy sampling fraction of 1.0 maximizes accuracy, although a fraction of 0.5 ($\text{fr}=0.5$) may be preferred when faster training is desired. We also observe that generating approximately 300 tokens in this task (denoted as tk in Table 5) during on-policy updates strikes an optimal balance between performance and efficiency, outperforming both 200-token and 400-token alternatives, while a generation temperature in the range of 0.8–0.9 is generally most effective.

Interestingly, the student model can sometimes surpass the teacher’s performance. In the two-stage training paradigm, employing larger teacher models (e.g., 14B rather than 7B or 3B) appears to provide additional benefits for the 1.5B student, although this trend is less pronounced in the single-stage FKL-only training.

Overall, these findings underscore the effectiveness of a two-stage training strategy: an initial supervised fine-tuning phase establishes a strong generative foundation, and subsequent on-policy distillation refines the model’s capabilities, leading to improved generalization and performance.

Ablation	Training Method	Val Loss
Baseline	SFT	0.2236
	3B-SFT	0.2081
	7B-SFT	0.1941
	14B-SFT	0.1771
Single Stage	FKL	0.2045
	FKL (3B)	0.2015
	JSD ($\beta = 0.5$)	0.2143
	RKL	0.2333
	oFKL	0.2107
Two Stages	SFT-SFT	0.2295
	SFT-oFKL	0.1982
	FKL-oFKL	0.1939
	FKL-oFKL (tk=200)	0.1910
	FKL-oFKL (tk=300)	0.1894
Different Teachers	FKL-oFKL (tk=400)	0.1910
	FKL-oFKL (tk=300, fr=0.5)	0.1917
	FKL (3B)-oFKL (3B)	0.1954
	FKL (3B)-oFKL (7B)	0.1918
	FKL (7B)-oFKL (7B)	0.1894
	FKL (14B)-oFKL (14B)	0.1863

Table 5: Validation losses for various training methods and ablations. Unless explicitly specified (e.g., FKL (3B) indicates distillation using the 3B-SFT model as the teacher), the default teacher is the 7B-SFT model.

5 Deployment

5.1 RecSys use case

SLM variants of the RecSys use case have been deployed to an A/B test.

Serving Infrastructure For all use cases, we benchmark and serve traffic using nodes with 256 CPU cores, 2TB of host memory and 8 NVIDIA H100 GPUs. As mentioned earlier, we deploy SGLang (version 0.4.1) as the serving engine. We use tensor parallelism to concurrently use more than 1 GPU for inference. To maximize performance, we employ FP8 quantization for both weights and activations and use FlashInfer [59] as the primary attention backend. Moreover, SGLang incorporates RadixAttention, which enables prefix caching for prompts sharing common prefixes.

Workloads For the RecSys workload, we follow the prompt structure outlined in Section 4.2 and utilize context lengths of 16k and 32k. Given the predictive nature of the task, the output length (i.e., the number of generated tokens) is set to 1, rendering the workload heavily reliant on the prefill phase. Consequently, optimizing the prefill stage is crucial for performance. For instance, prefix caching substantially improves prefill (and decode) times when a prompt’s key (K) and value (V) tensors for its shared prefix have already been processed. In cases where there are k candidate items to be ranked for a member m , k prompts are served. These prompts share a long prefix containing the user information and historical item interactions. Once one prompt is served, its KV tensors are cached, allowing subsequent prompts for the same member to reuse the cached data—a process we refer to as a hot prefill.

Metrics We use two key metrics - time to first token (TTFT) and time per output token (TPOT). For prediction tasks, which are prefill-intensive, TTFT is the primary metric as it reflects the duration of the prefill phase. For generative tasks, both TTFT and TPOT are important. Additionally, we report the total serving throughput for various context lengths.

Results In terms of quality, the models under consideration perform similarly since their AUCs are similar. For performance, we report TTFT and throughput measurements for both 16k and 32k context lengths. P99 TTFT results for a workload with 1 QPS (i.e., $m = 1$) and 1 or more prompt per member (i.e., $k = 1$ or more) can be found in Figure 4 (detailed p50, p99 and throughput numbers can be found in Tables 9, 10 and 11 in Appendix A.2). From the figure and the tables, we can conclude that latency drops drastically as model size becomes smaller. Serving traffic with 32k context is significantly slower than serving traffic with 16k context. Setting k more than 1 doesn’t hurt latency much, because of KV caching.

To better understand the effect of model pruning on inference latency, we present the break down of forward pass for a single layer in Figure 5. As it can be seen, the attention step is the main latency bottleneck. Our structured pruning of the attention heads improves the attention latency by about 40% which in turn results in more than 28% speed up in prefill latency.

5.2 Generative use case

The reasoning task outlined in Section 4.3 was launched online for a 1% A/B test. Results are outlined in Table 6. KD, along with data changes, helped the model improve by 20.29% on an internal quality metric (IQM). We also discuss deployment lessons from a

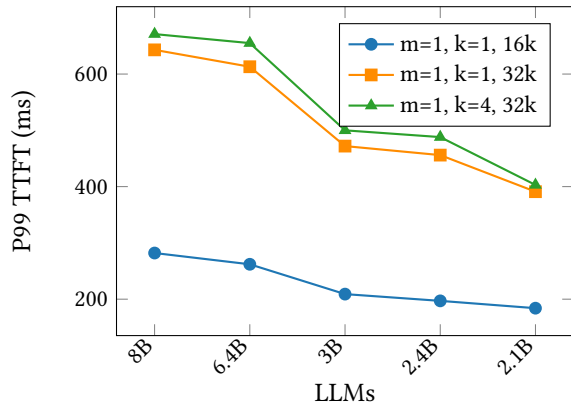


Figure 4: P99 TTFT (ms) for various LLMs

Model	IQM (%)
KD Model	+20.29%

Table 6: Online A/B test results for reasoning task.

generative use case to study the effect of different quantization schemes on model inference speed and accuracy.

Serving Infrastructure Our setup is mostly similar to Section 5.1. However, in addition to using NVIDIA H100 GPUs, we also study the effect of using older NVIDIA A100 GPUs. To this end, we use the vLLM backend (version 0.6.1) for serving. We use 1 GPU for serving (TP=1).

Workloads The workload here consists of prompts with varying lengths, averaging to 3.8k tokens per request, with 1 request per second. The output generation is capped to 2k tokens. As we focus on a generative task here, we report both TTFT and TPOT. We study a Llama3-based model with the 8B size, and consider several serving scenarios with or without quantization using different hardware.

Performance Results The inference speed results are reported in Table 7. Using the state-of-the-art H100 GPUs results in faster inference (both in terms of TTFT and TPOT) compared to A100 GPUs. In particular, we observe that FP8 serving with H100s leads to the smallest TTFT and TPOT. However, limiting our comparisons to A100 GPUs, we see that using INT8 (W8A8) quantization results in significant reduction of both TTFT and TPOT. On the other hand, INT4 (w4A16) quantization actually increases TTFT, while decreasing TPOT. For generative task with long output sequences, we observe that W4A16 has smaller latency. In summary, we have observed that using higher-end hardware such as H100 leads to the most speed-ups. When such hardware is not available, for generative tasks with long output sequences, W4A16 has the most speed-up, while W8A8 can be more appropriate for prefill-heavy tasks. For the sake of completeness, we present a brief comparison of quantization methods in terms of accuracy in Appendix A.1.

6 Conclusion

In this paper, we highlight the importance of training and deploying small language models (SLMs) for real-world industry use cases.

Model	P50 TTFT (ms)	P50 TPOT (ms)	GPU
FP16	136	10.3	H100
FP8	122	9.4	H100
FP16	332	18.3	A100
W8A8 (INT)	227	12.9	A100
W4A16 (INT)	389	11.2	A100

Table 7: Comparison of different quantization methods for the Llama-3 8B model.

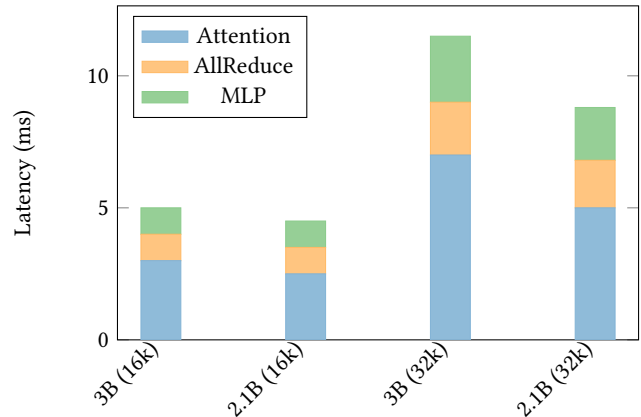


Figure 5: Latency breakdown of a single Transformer block for pruned and unpruned models. As context size increases, attention becomes a major bottleneck.

We specifically drill into model distillation and compression techniques, carefully dissecting the value added by each technique for model generalization. After creating high-quality SLMs, we also detail deployment lessons learned in terms of latency and hardware efficiency. Future directions could include on-policy data-based training for more robust distillation and extending pruning to the attention parts of the transformer blocks.

References

- [1] Josh Achiam, Steven Adler, Sandhini Agarwal, Lama Ahmad, Ilge Akkaya, Florencia Leoni Aleman, Diogo Almeida, Janko Altmenschmidt, Sam Altman, Shyamal Anadkat, et al. 2023. Gpt-4 technical report. *arXiv preprint arXiv:2303.08774* (2023).
- [2] Rishabh Agarwal, Nino Vieillard, Yongchao Zhou, Piotr Stanczyk, Sabela Ramos Garea, Matthieu Geist, and Olivier Bachem. 2024. On-policy distillation of language models: Learning from self-generated mistakes. In *The Twelfth International Conference on Learning Representations*.
- [3] Saleh Ashkboos, Iman Mirzadeh, Keivan Alizadeh, Mohammad Hossein Sekhavat, Moin Nabi, Mehrdad Farajtabar, and Fartash Faghri. 2024. Computational Bottlenecks of Training Small-scale Large Language Models. *arXiv preprint arXiv:2410.19456* (2024).
- [4] Kayhan Behdin, Ayan Acharya, Aman Gupta, Qingquan Song, Siyu Zhu, Sathiya Keerthi, and Rahul Mazumder. 2023. QuantEase: Optimization-based Quantization for Language Models. *arXiv e-prints* (2023), arXiv-2309.
- [5] Riade Benbaki, Wenyu Chen, Xiang Meng, Hussein Hazim, Natalia Ponomareva, Zhe Zhao, and Rahul Mazumder. 2023. Fast as chita: Neural network pruning with combinatorial optimization. In *International Conference on Machine Learning*. PMLR, 2031–2049.
- [6] Yonatan Bisk, Rowan Zellers, Jianfeng Gao, Yejin Choi, et al. 2020. Piqa: Reasoning about physical commonsense in natural language. In *Proceedings of the AAAI conference on artificial intelligence*, Vol. 34. 7432–7439.

- [7] Tom Brown, Benjamin Mann, Nick Ryder, Melanie Subbiah, Jared D Kaplan, Prafulla Dhariwal, Arvind Neelakantan, Pranav Shyam, Girish Sastry, Amanda Askell, et al. 2020. Language models are few-shot learners. *Advances in neural information processing systems* 33 (2020), 1877–1901.
- [8] Aakanksha Chowdhery, Sharan Narang, Jacob Devlin, Maarten Bosma, Gaurav Mishra, Adam Roberts, Paul Barham, Hyung Won Chung, Charles Sutton, Sebastian Gehrmann, et al. 2023. Palm: Scaling language modeling with pathways. *Journal of Machine Learning Research* 24, 240 (2023), 1–113.
- [9] Peter Clark, Isaac Cowhey, Oren Etzioni, Tushar Khot, Ashish Sabharwal, Carissa Schoenick, and Oyvind Tafjord. 2018. Think you have solved question answering? try arc, the ai2 reasoning challenge. *arXiv preprint arXiv:1803.05457* (2018).
- [10] Yun Dai, Tejas Dharamsi, Pin-Lun Hsu, Tao Song, and Hamed Firooz. 2024. Enhancing stability for large models training in constrained bandwidth networks. In *Workshop on Efficient Systems for Foundation Models II@ ICML2024*.
- [11] Sumit Kumar Dam, Choong Seon Hong, Yu Qiao, and Chaoning Zhang. 2024. A complete survey on llm-based ai chatbots. *arXiv preprint arXiv:2406.16937* (2024).
- [12] Jacob Devlin. 2018. Bert: Pre-training of deep bidirectional transformers for language understanding. *arXiv preprint arXiv:1810.04805* (2018).
- [13] Abhimanyu Dubey, Abhinav Jauhri, Abhinav Pandey, Abhishek Kadian, Ahmad Al-Dahle, Aiesha Letman, Akhil Mathur, Alan Schelten, Amy Yang, Angela Fan, et al. 2024. The llama 3 herd of models. *arXiv preprint arXiv:2407.21783* (2024).
- [14] Hamed Firooz, Maziar Sanjabi, Adrian Enghardt, Aman Gupta, Ben Levine, Dre Olgiati, Gungor Polatkan, Iulia Melnychuk, Karthik Ramgopal, Kirill Talanin, et al. 2025. 360Brew: A Decoder-only Foundation Model for Personalized Ranking and Recommendation. *arXiv preprint arXiv:2501.16450* (2025).
- [15] Elias Frantar and Dan Alistarh. 2023. Sparsegpt: Massive language models can be accurately pruned in one-shot. In *International Conference on Machine Learning*. PMLR, 10323–10337.
- [16] Elias Frantar, Saleh Ashkboos, Torsten Hoefer, and Dan Alistarh. 2022. Gptq: Accurate post-training quantization for generative pre-trained transformers. *arXiv preprint arXiv:2210.17323* (2022).
- [17] Yuxian Gu, Li Dong, Furu Wei, and Minlie Huang. 2024. MiniLLM: Knowledge distillation of large language models. In *The Twelfth International Conference on Learning Representations*.
- [18] Tom Gunter, Zirui Wang, Chong Wang, Ruoming Pang, Andy Narayanan, Anon Zhang, Bowen Zhang, Chen Chen, Chung-Cheng Chiu, David Qiu, et al. 2024. Apple intelligence foundation language models. *arXiv preprint arXiv:2407.21075* (2024).
- [19] Daya Guo, Dejian Yang, Haowei Zhang, Junxiao Song, Ruoyu Zhang, Runxin Xu, Qihao Zhu, Shiroong Ma, Peiyi Wang, Xiao Bi, et al. 2025. Deepseek-r1: Incentivizing reasoning capability in llms via reinforcement learning. *arXiv preprint arXiv:2501.12948* (2025).
- [20] Babak Hassibi, David G Stork, and Gregory J Wolff. 1993. Optimal brain surgeon and general network pruning. In *IEEE international conference on neural networks*. IEEE, 293–299.
- [21] Geoffrey Hinton. 2015. Distilling the Knowledge in a Neural Network. *arXiv preprint arXiv:1503.02531* (2015).
- [22] Jordan Hoffmann, Sebastian Borgeaud, Arthur Mensch, Elena Buchatskaya, Trevor Cai, Eliza Rutherford, Diego de Las Casas, Lisa Anne Hendricks, Johannes Welbl, Aidan Clark, et al. 2022. Training compute-optimal large language models. *arXiv preprint arXiv:2203.15556* (2022).
- [23] Pin-Lun Hsu, Yun Dai, Vignesh Kothapalli, Qingquan Song, Shao Tang, Siyu Zhu, Steven Shimizu, Shivam Sahni, Haowen Ning, and Yanming Chen. 2024. Liger kernel: Efficient triton kernels for llm training. *arXiv preprint arXiv:2410.10989* (2024).
- [24] Albert Q Jiang, Alexandre Sablayrolles, Arthur Mensch, Chris Bamford, Devendra Singh Chaplot, Diego de las Casas, Florian Bressand, Gianna Lengyel, Guillaume Lample, Lucile Saulnier, et al. 2023. Mistral 7B. *arXiv preprint arXiv:2310.06825* (2023).
- [25] Woojeong Jin, Maziar Sanjabi, Shaoliang Nie, Liang Tan, Xiang Ren, and Hamed Firooz. 2021. Modality-specific distillation. In *Proceedings of the Third Workshop on Multimodal Artificial Intelligence*. 42–53.
- [26] Jared Kaplan, Sam McCandlish, Tom Henighan, Tom B Brown, Benjamin Chess, Rewon Child, Scott Gray, Alec Radford, Jeffrey Wu, and Dario Amodei. 2020. Scaling laws for neural language models. *arXiv preprint arXiv:2001.08361* (2020).
- [27] Yoon Kim and Alexander M Rush. 2016. Sequence-level knowledge distillation. *arXiv preprint arXiv:1606.07947* (2016).
- [28] Jongwoo Ko, Sungyun Kim, Tianyi Chen, and Se-Young Yun. 2024. Distillm: Towards streamlined distillation for large language models. *arXiv preprint arXiv:2402.03898* (2024).
- [29] Eldar Kurtić, Elias Frantar, and Dan Alistarh. 2024. Ziplm: Inference-aware structured pruning of language models. *Advances in Neural Information Processing Systems* 36 (2024).
- [30] Woosuk Kwon, Sehoon Kim, Michael W Mahoney, Joseph Hassoun, Kurt Keutzer, and Amir Gholami. 2022. A fast post-training pruning framework for transformers. *Advances in Neural Information Processing Systems* 35 (2022), 24101–24116.
- [31] Woosuk Kwon, Zhuohan Li, Siyuan Zhuang, Ying Sheng, Lianmin Zheng, Cody Hao Yu, Joseph E. Gonzalez, Hao Zhang, and Ion Stoica. 2023. Efficient Memory Management for Large Language Model Serving with PagedAttention. In *Proceedings of the ACM SIGOPS 29th Symposium on Operating Systems Principles*.
- [32] Yann LeCun, John Denker, and Sara Solla. 1989. Optimal brain damage. *Advances in neural information processing systems* 2 (1989).
- [33] Jiacheng Li, Ming Wang, Jin Li, Jimiao Fu, Xin Shen, Jingbo Shang, and Julian McAuley. 2023. Text is all you need: Learning language representations for sequential recommendation. In *Proceedings of the 29th ACM SIGKDD Conference on Knowledge Discovery and Data Mining*. 1258–1267.
- [34] Xiaopeng Li, Lixin Su, Pengyue Jia, Xiangyu Zhao, Suqi Cheng, Junfeng Wang, and Dawei Yin. 2023. Agent4ranking: Semantic robust ranking via personalized query rewriting using multi-agent llm. *arXiv preprint arXiv:2312.15450* (2023).
- [35] Aixian Liu, Bei Feng, Bing Xue, Bingxuan Wang, Bochao Wu, Chengda Lu, Cheng-gang Zhao, Chengqi Deng, Chenyu Zhang, Chong Ruan, et al. 2024. Deepseek-v3 technical report. *arXiv preprint arXiv:2412.19437* (2024).
- [36] Xiang Meng, Kayhan Behdin, Haoyue Wang, and Rahul Mazumder. 2024. ALPS: Improved Optimization for Highly Sparse One-Shot Pruning for Large Language Models. *arXiv preprint arXiv:2406.07831* (2024).
- [37] Xiang Meng, Shibal Ibrahim, Kayhan Behdin, Hussein Hazimeh, Natalia Ponomareva, and Rahul Mazumder. 2024. OSSCAR: One-Shot Structured Pruning in Vision and Language Models with Combinatorial Optimization. *arXiv preprint arXiv:2403.12983* (2024).
- [38] Aaron Mueller, Kanika Narang, Lambert Mathias, Qifan Wang, and Hamed Firooz. 2023. Meta-training with demonstration retrieval for efficient few-shot learning. *arXiv preprint arXiv:2307.00119* (2023).
- [39] Saurav Muralidharan, Sharath Turuvekere Sreenivas, Raviraj Joshi, Marcin Chochowski, Mostafa Patwary, Mohammad Shoeybi, Bryan Catanzaro, Jan Kautz, and Pavlo Molchanov. 2024. Compact Language Models via Pruning and Knowledge Distillation. *arXiv preprint arXiv:2407.14679* (2024).
- [40] Saurav Muralidharan, Sharath Turuvekere Sreenivas, Raviraj Joshi, Marcin Chochowski, Mostafa Patwary, Mohammad Shoeybi, Bryan Catanzaro, Jan Kautz, and Pavlo Molchanov. 2024. LLM Pruning and Distillation in Practice: The Minitron Approach. *arXiv preprint arXiv:2408.11796* (2024).
- [41] NVIDIA. 2024. TensorRT-LLM. GitHub: <https://github.com/NVIDIA/TensorRT-LLM>.
- [42] Aldo Pareja, Nikhil Shivakumar Nayak, Hao Wang, Krishnateja Killamsetty, Shivchander Sudalairaj, Wenlong Zhao, Seungwook Han, Abhishek Bhandwadar, Guangxuan Xu, Kai Xu, et al. 2024. Unveiling the Secret Recipe: A Guide For Supervised Fine-Tuning Small LLMs. *arXiv preprint arXiv:2412.13337* (2024).
- [43] Zhen Qin, Rolf Jagerman, Kai Hui, Honglei Zhuang, Junru Wu, Le Yan, Jiaming Shen, Tianqi Liu, Jialu Liu, Donald Metzler, et al. 2023. Large language models are effective text rankers with pairwise ranking prompting. *arXiv preprint arXiv:2306.17563* (2023).
- [44] Colin Raffel, Noam Shazeer, Adam Roberts, Katherine Lee, Sharan Narang, Michael Matena, Yanqi Zhou, Wei Li, and Peter J Liu. 2020. Exploring the limits of transfer learning with a unified text-to-text transformer. *Journal of machine learning research* 21, 140 (2020), 1–67.
- [45] Samyam Rajbhandari, Jeff Rasley, Olatunji Ruwase, and Yuxiong He. 2020. Zero: Memory optimizations toward training trillion parameter models. In *SC20: International Conference for High Performance Computing, Networking, Storage and Analysis*. IEEE, 1–16.
- [46] Aditya Ramesh, Prafulla Dhariwal, Alex Nichol, Casey Chu, and Mark Chen. 2022. Hierarchical text-conditional image generation with clip latents. *arXiv preprint arXiv:2204.06125* 1, 2 (2022), 3.
- [47] Mingjie Sun, Zhuang Liu, Anna Bair, and J Zico Kolter. 2023. A simple and effective pruning approach for large language models. *arXiv preprint arXiv:2306.11695* (2023).
- [48] Gemini Team, Rohan Anil, Sebastian Borgeaud, Jean-Baptiste Alayrac, Jiahui Yu, Radu Soricut, Johan Schalkwyk, Andrew M Dai, Anja Hauth, Katie Millican, et al. 2023. Gemini: a family of highly capable multimodal models. *arXiv preprint arXiv:2312.11805* (2023).
- [49] MLC team. 2023-2025. MLC-LLM. <https://github.com/mlc-ai/mlc-llm>
- [50] Philippe Tillet, Hsiang-Tsung Kung, and David Cox. 2019. Triton: an intermediate language and compiler for tiled neural network computations. In *Proceedings of the 3rd ACM SIGPLAN International Workshop on Machine Learning and Programming Languages*. 10–19.
- [51] Lewis Tunstall, Edward Beeching, Nathan Lambert, Nazneen Rajani, Kashif Rasul, Younes Belkada, Shengyi Huang, Leandro von Werra, Clémentine Fourrier, Nathan Habib, et al. 2023. Zephyr: Direct distillation of llm alignment. *arXiv preprint arXiv:2310.16944* (2023).
- [52] Guanhua Wang, Heyang Qin, Sam Ade Jacobs, Connor Holmes, Samyam Rajbhandari, Olatunji Ruwase, Feng Yan, Lei Yang, and Yuxiong He. 2023. Zero++: Extremely efficient collective communication for giant model training. *arXiv preprint arXiv:2306.10209* (2023).
- [53] Liang Wang, Nan Yang, Xiaolong Huang, Binxing Jiao, Linjun Yang, Daxin Jiang, Rangan Majumder, and Furu Wei. 2022. Text embeddings by weakly-supervised

Model	ARC-c	ARC-e	PIQA
FP16	0.5299	0.8136	0.7982
FP8	0.5179	0.8056	0.7922
W8A8-INT	0.5171	0.8123	0.7954
W4A16-INT-GPTQ	0.436	0.7306	0.7437
W4A16-INT-QuantEase	0.5077	0.8068	0.7954

Table 8: Comparison of different quantization schemes with the Llama 3.1 8B Instruct model.

- contrastive pre-training. *arXiv preprint arXiv:2212.03533* (2022).
- [54] Liang Wang, Nan Yang, Xiaolong Huang, Linjun Yang, Rangan Majumder, and Furu Wei. 2023. Improving text embeddings with large language models. *arXiv preprint arXiv:2401.00368* (2023).
- [55] Jason Wei, Xuezhi Wang, Dale Schuurmans, Maarten Bosma, Fei Xia, Ed Chi, Quoc V Le, Denny Zhou, et al. 2022. Chain-of-thought prompting elicits reasoning in large language models. *Advances in neural information processing systems* 35 (2022), 24824–24837.
- [56] Guangxuan Xiao, Ji Lin, Mickael Seznec, Hao Wu, Julien Demouth, and Song Han. 2023. Smoothquant: Accurate and efficient post-training quantization for large language models. In *International Conference on Machine Learning*. PMLR, 38087–38099.
- [57] Wenda Xu, Rujun Han, Zifeng Wang, Long T Le, Dhruv Madeka, Lei Li, William Yang Wang, Rishabh Agarwal, Chen-Yu Lee, and Tomas Pfister. 2024. Speculative Knowledge Distillation: Bridging the Teacher-Student Gap Through Interleaved Sampling. *arXiv preprint arXiv:2410.11325* (2024).
- [58] An Yang, Baosong Yang, Beichen Zhang, Binyuan Hui, Bo Zheng, Bowen Yu, Chengyuan Li, Dayiheng Liu, Fei Huang, Haoran Wei, et al. 2024. Qwen2. 5 technical report. *arXiv preprint arXiv:2412.15115* (2024).
- [59] Zihao Ye, Lequn Chen, Ruihang Lai, Wuwei Lin, Yineng Zhang, Stephanie Wang, Tianqi Chen, Baris Kasikci, Vinod Grover, Arvind Krishnamurthy, and Luis Ceze. 2025. FlashInfer: Efficient and Customizable Attention Engine for LLM Inference Serving. *arXiv preprint arXiv:2501.01005* (2025). <https://arxiv.org/abs/2501.01005>
- [60] Wayne Xin Zhao, Jing Liu, Ruiyang Ren, and Ji-Rong Wen. 2024. Dense text retrieval based on pretrained language models: A survey. *ACM Transactions on Information Systems* 42, 4 (2024), 1–60.
- [61] Lianmin Zheng, Liangsheng Yin, Zhiqiang Xie, Chuyue Sun, Jeff Huang, Cody Hao Yu, Shiyi Cao, Christos Kozyrakis, Ion Stoica, Joseph E Gonzalez, et al. 2024. Sglang: Efficient execution of structured language model programs. *arXiv preprint arXiv:2312.07104* (2024).
- [62] Yongchao Zhou, Kaifeng Lyu, Ankit Singh Rawat, Aditya Krishna Menon, Afshin Rostamizadeh, Sanjiv Kumar, Jean-François Kagy, and Rishabh Agarwal. 2023. Distillspec: Improving speculative decoding via knowledge distillation. *arXiv preprint arXiv:2310.08461* (2023).
- [63] Xunyu Zhu, Jian Li, Yong Liu, Can Ma, and Weiping Wang. 2023. A Survey on Model Compression for Large Language Models. *arXiv preprint arXiv:2308.07633* (2023).

A Appendix

A.1 Comparison of Quantization Methods

We present a comparison of different quantization methods. We use the Meta Llama 3.1 8B Instruct model, and quantize the model using 1024 samples from the open source C4 [44] dataset as the calibration set. We report the zero-shot accuracy of the model on three open-source tasks PIQA [6] and ARC easy/challenge [9]. We compare W8A8 quantization with SmoothQuant [56], FP8 quantization on H100 GPUs, and W4A16 quantization with GPTQ [16] and QuantEase [4]. The results are shown in Table 8. We see that 8-bit quantization generally has a small loss of accuracy. On the other hand, GPTQ with W4A16 shows some model quality degradation. However, using QuantEase for better optimization helps to reduce the model quality gap. In our internal experiments, we have observed similar trends when comparing different methods.

A.2 Extra tables for Section 5

Model	P50 TTFT (ms)	P99 TTFT (ms)	Throughput
FM	1032	1039	14127
8b	271	282	14121
6.4B	256	269	14121
3B	195	209	14121
2.4B	189	197	14122
2.1B	171	184	14110

Table 9: Results for $m = 1, k = 1$ for 16k context length using 4 GPUs (tp=4).

Model	P50 TTFT (ms)	P99 TTFT (ms)	Throughput
FM	407661	45791	15740
8b	626	643	28427
6.4B	600	613	28427
3B	452	472	28423
2.4B	437	456	28422
2.1B	367	391	28420

Table 10: Results for $m = 1, k = 1$ for 32k context length using 4 GPUs (tp = 4).

Model	P50 TTFT (ms)	P99 TTFT (ms)	Throughput
FM	179483	370376	45081
8b	646	671	115568
6.4B	626	655	115560
3B	477	500	115546
2.4B	465	488	115544
2.1B	378	403	115520

Table 11: Results for $m = 1$, and $k = 4$ for $32k$ context length using 4 GPUs (tp=4).